# Los Alamos
NATIONAL LABORATORY
# memorandum

Los Alamos Neutron Science Center, LANSCE-1
Accelerator Physics and Engineering Group

*To/MS:* Distribution
*From/MS:* Robert Garnett, H817
*Phone/Fax:* 5-2835/5-2904
*Symbol:* LANSCE-1:00-052
*Date:* June 26, 2000
*Email:* rgarnett@lanl.gov

**SUBJECT: SNS MEBT Steering Requirements and DTL Tank 1 Acceptance**

Simulations have been completed to determine the amount of MEBT steering required to map out the SNS DTL Tank 1 acceptance. It will be desirable to use the beam steering capability in the MEBT to scan the beam across the linac aperture and measure the beam transmission at the output of Tank 1 during the commissioning studies. Additionally, the acceptance of the tank has been determined. The results are given below.

## MEBT Steering

The MEBT layout is shown in Figure 1. Steering in the MEBT will be done in six of the 14 MEBT quads: QM1, QM4, QM5, QM10, QM11, and QM14. Energizing separate steering coils in each of these magnets will allow simultaneous steering in both x and y at each location. The specifications for the steerers are shown in Table 1 as given to me by John Staples (LBNL). He has tested some of these magnets and expects to be able to get deflecting fields on the order of 4-5 mrad, which is higher than what was designed for. Based on the information in Table 1, the GL product required to give a bend angle of 4 mrad is calculated to be 911.63 Gauss-cm.

Table 1 - MEBT Steerer Specifications

| Magnet | R-bore (cm) | R-pole-tip (cm) | Leff Lcore+R-pole-tip (cm) | Design Gradient | Design Bend |
|---|---|---|---|---|---|
| QM1, QM4, QM11, QM14 | 1.5 | 1.6 | 6.1 | 60.9 Gauss | ± 1.63 mrad |
| QM5-QM10 | 2.0 | 2.1 | 6.6 | 46.4 Gauss | ± 1.34 mrad |

In this study, we have assumed that all steering to measure acceptance will be done using the final two steering quads, QM11 and/or QM14. Figure 2 shows the beam dynamics results using a 10,000-macroparticle distribution to map out the acceptance using only QM14. The RFQ output beam was transported through both the MEBT and Tank 1 of the DTL. The beam transmission at the end of Tank 1 is shown as a function of QM14 x- and y-steering strengths. A spline-fit to the simulated transmission data is also shown to aid the eye. These results indicate that much stronger steering is required than is presently planned for in the MEBT. Figure 3 shows the Tank 1 output transmission as a function of QM14 x-steering only and also for combined QM11 + QM14 x-steering. As can be seen, very little is gained by using a combination of these two steerers.

The effects of varying the QM14 quadrupole gradient were also examined. Figure 4 shows the Tank 1 transmission as a function of QM14 gradient variations (± 50%). As can be seen, the transmission is relatively insensitive to large variations to the gradient. Since it will also be possible to measure beam profiles at the end of Tank1 during commissioning, the variation in rms beam size as a function of QM14 quadrupole gradient was also examined. Figure 5 shows the results. Unfortunately, the rms beam size is also relatively insensitive to these variations.

**Tank 1 Acceptance**

The Tank 1 acceptance was calculated by using grids of particles in both real space and in longitudinal phase space as input to the PARMILA code. Knowing the acceptance of Tank 1 is useful for determining the requirements of the emittance gear and wire-scanners to be used for commissioning and also to confirm the previously discussed steering results.

Figure 6 shows the input phase space plots (acceptance plots) of the macroparticles that were transported through Tank 1. All MEBT quads were set to their expected nominal values and all steerers were off. The angular acceptance is approximately ±40 mrad and ±50 mrad in x' and y', respectively. In Figure 2, a significant fall-off in the transmission (to 25%) is not seen until the steering strength is approximately 5000 G-cm. This is equivalent to a 22-mrad deflection based on scaling from the Table 1 parameters. Figure 7 shows the Tank 1 output phase space distributions resulting from the acceptance calculation (grid inputs). These results are consistent with the multi-particle steering simulation results discussed earlier. For comparison, Figure 8 shows the Tank 1 output phase space distributions expected from the RFQ distribution.

**Recommendations**

Stronger steering is required at the end of the MEBT. Either QM14 should be redesigned to provide a GL-product of 5000 G-cm or an additional dedicated steering magnet should be placed near the end of the MEBT. I suspect that there is no space for an additional magnet. If it is not possible to significantly modify the quad design, it may be useful to study the transport of the beam with QM12-QM14 off. It may be possible to drift the beam from QM11, with no additional focusing, to the DTL. These quads would only be off during the acceptance mapping. For this situation, the steering strength required, for a larger beam displacement at the DTL entrance, should be significantly smaller due to the longer lever-arm allowed before injection into the DTL.

The wire scanner that will be provided in the inter-tank space should be able to measure beam profiles over the range ± 1.5cm. The emittance gear used during commissioning should be able to provide x and y measurements over that same range along with angle measurements of ± 30 mrad.

RWG:amg

Distribution:
R. Garnett, LANSCE-1, H817
S. Nath, SNS-PO, H824
R. Shafer, LANSCE-1, H808
J. Stovall, SNS-PO, H824
B. Miller, SNS-PO, H824
A. Jason, LANSCE-1, H817
LANSCE-1 File

Pass to [illegible] when you are done

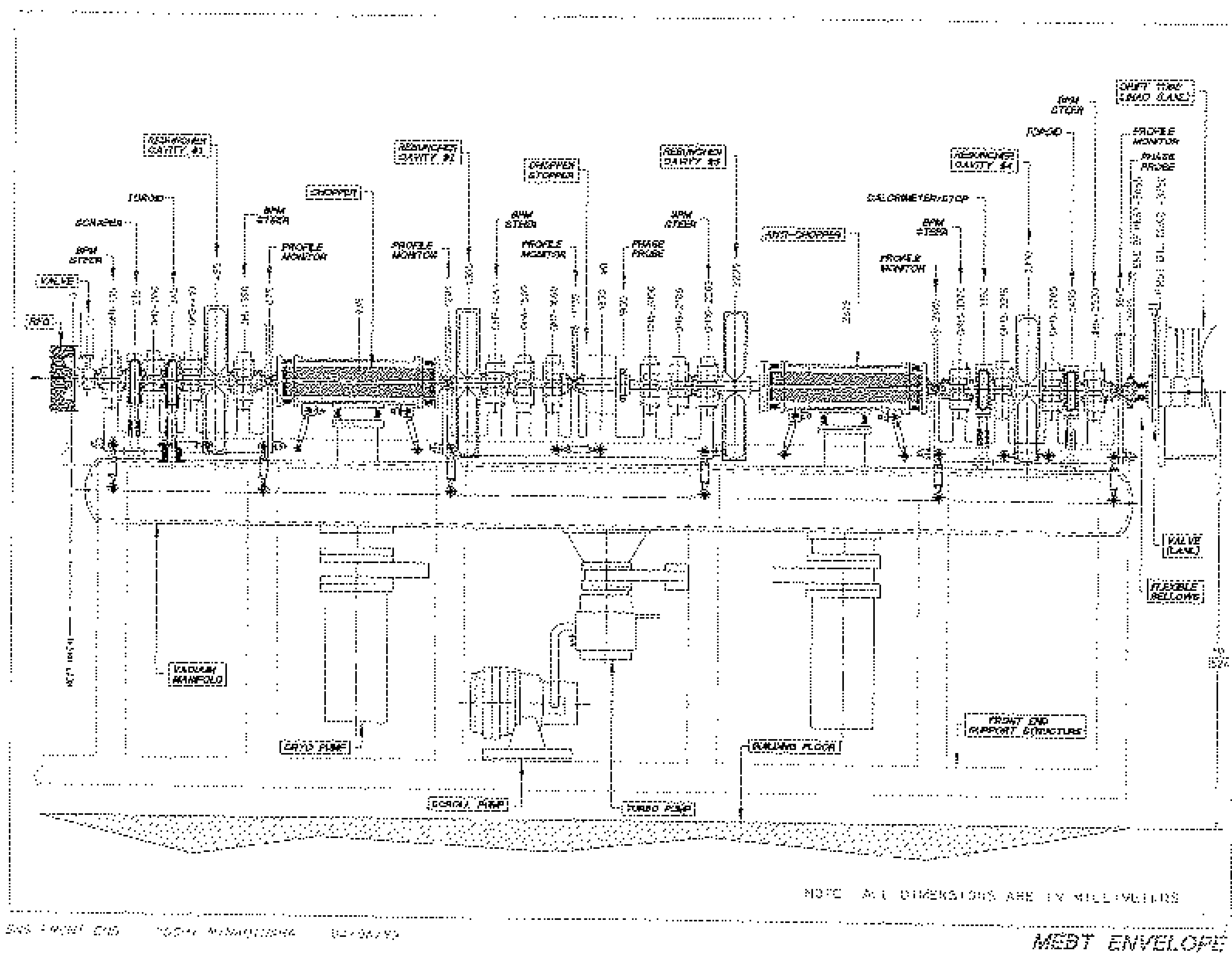


Figure 1 – SNS MEBT Layout

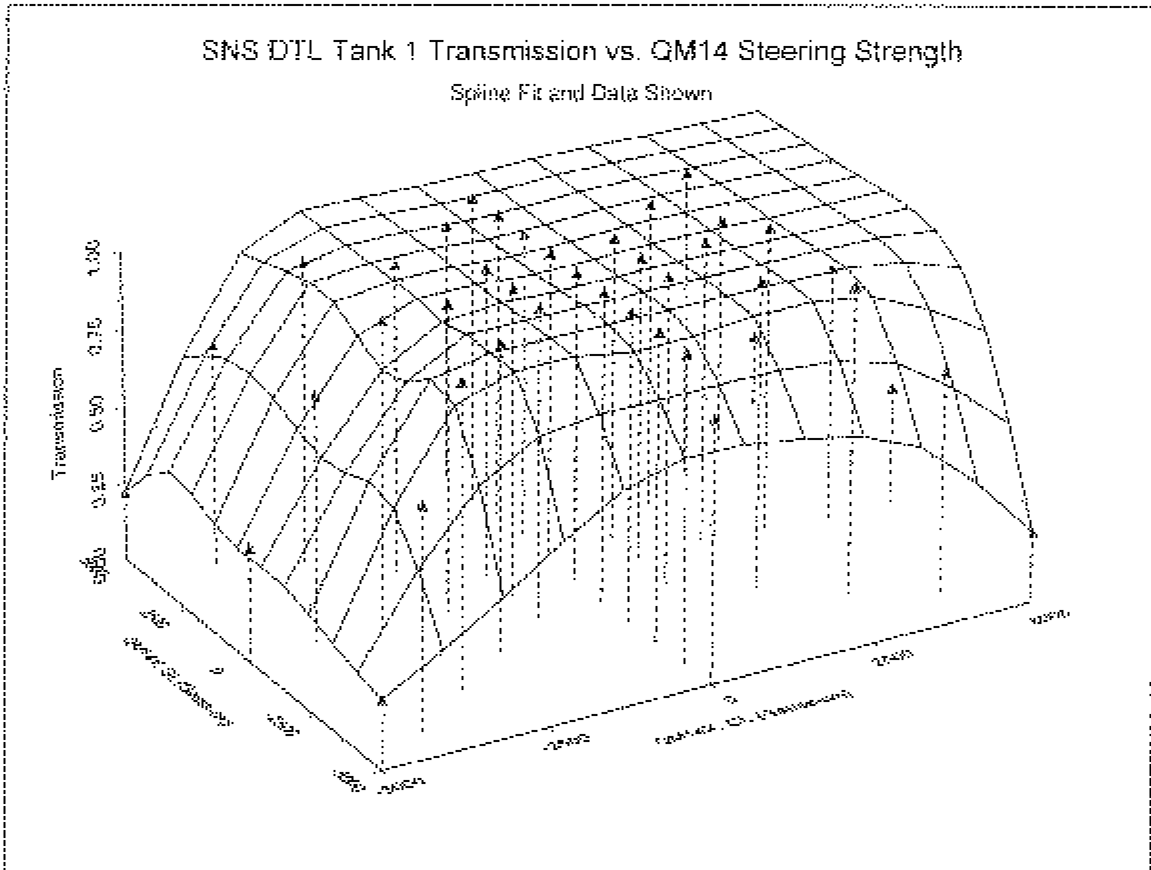


Figure 2 – DTL Tank 1 transmission as a function of QM14 x and y steering strength.

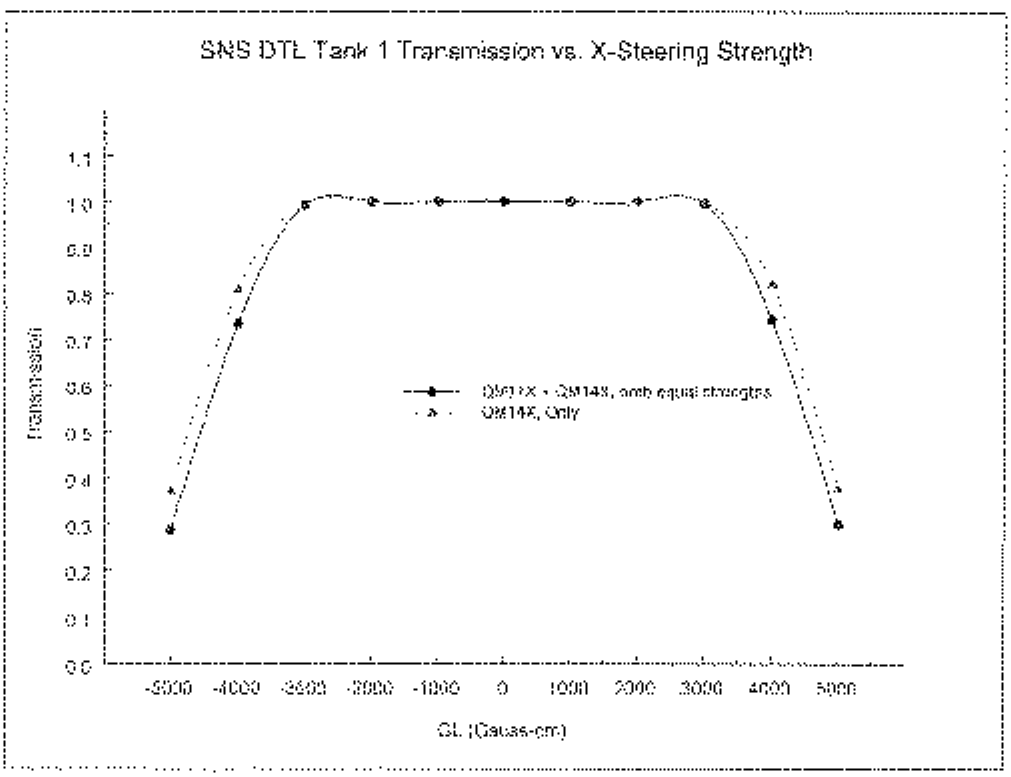


Figure 3 – Tank 1 transmission as a function of QM11+QM14 steering.

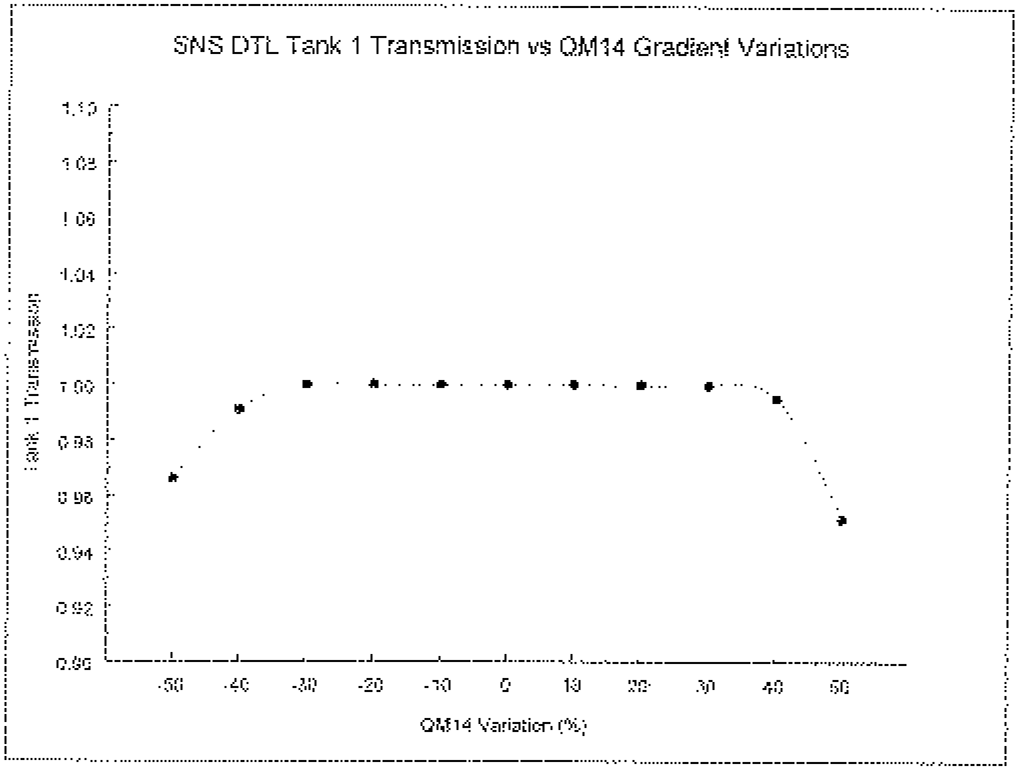


Figure 4 – Tank1 transmission as a function of QM14 gradient variations

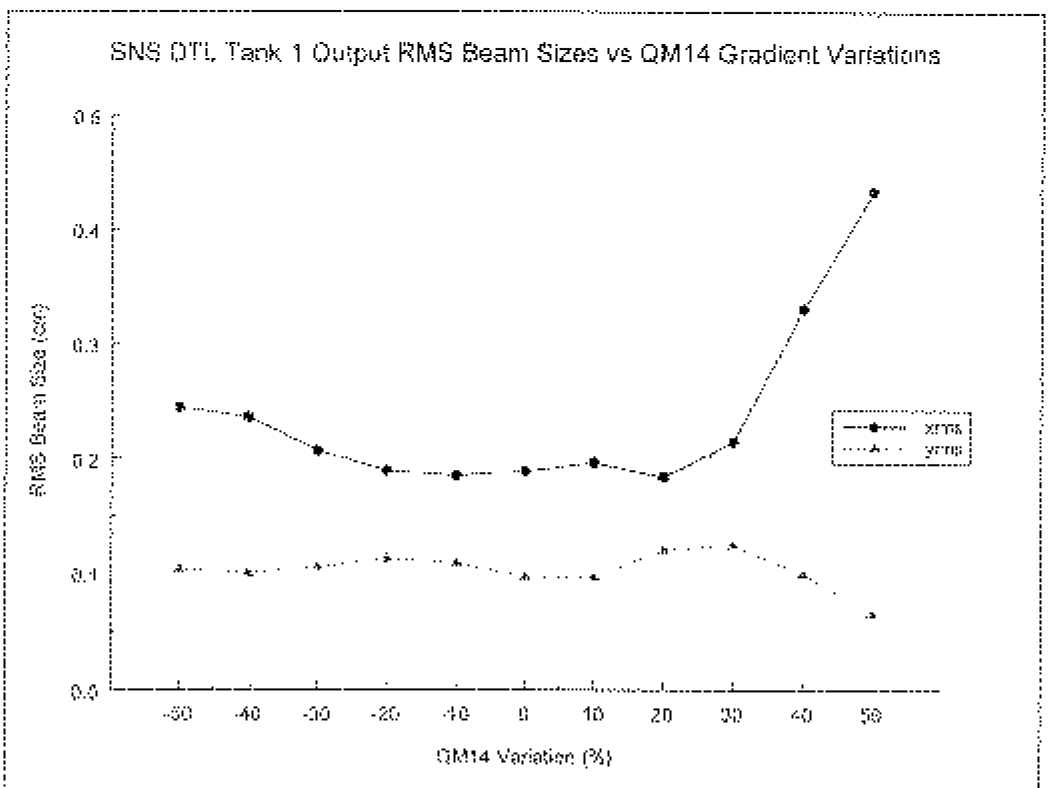


Figure 5 – Tank 1 output rms beam size as a function of QM14 gradient variations.

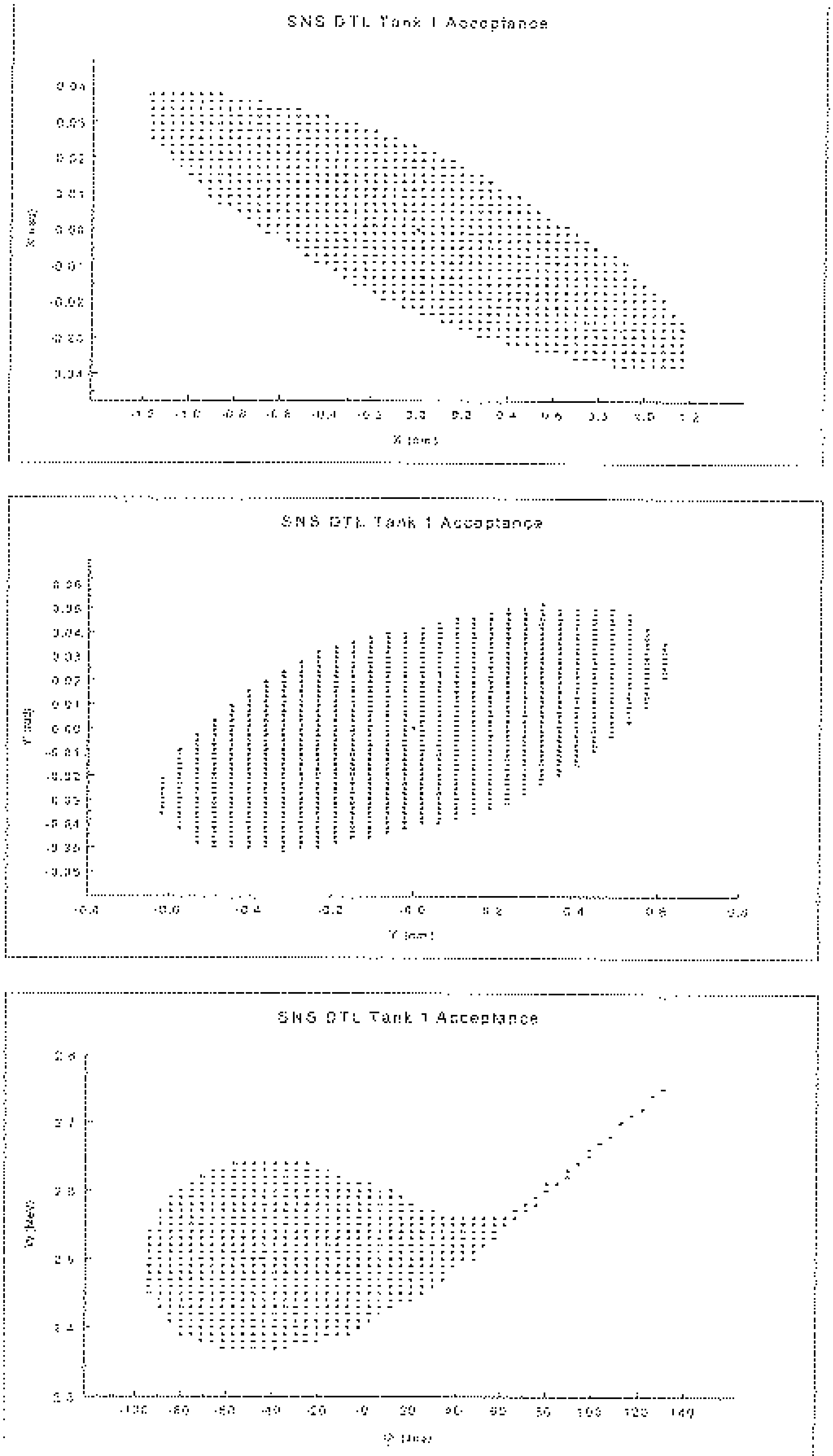


Figure 6 – DTL Tank 1 acceptance plots.

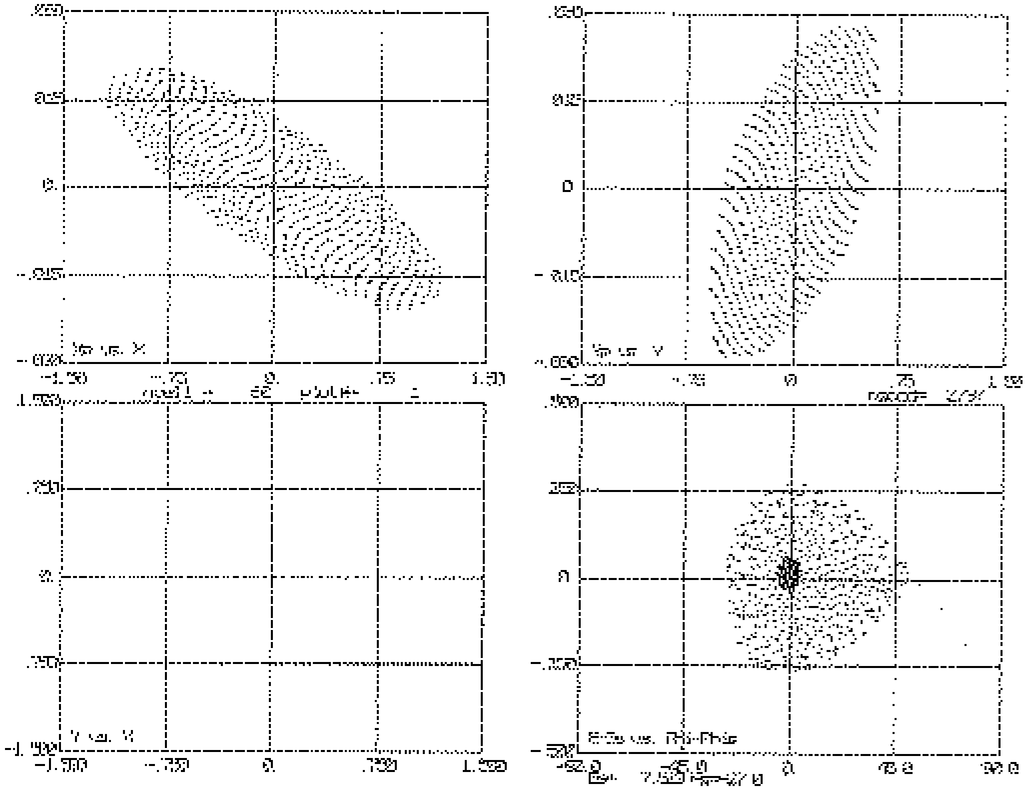

Figure 7 -- Tank 1 output phase-space distributions using the grid input beams.

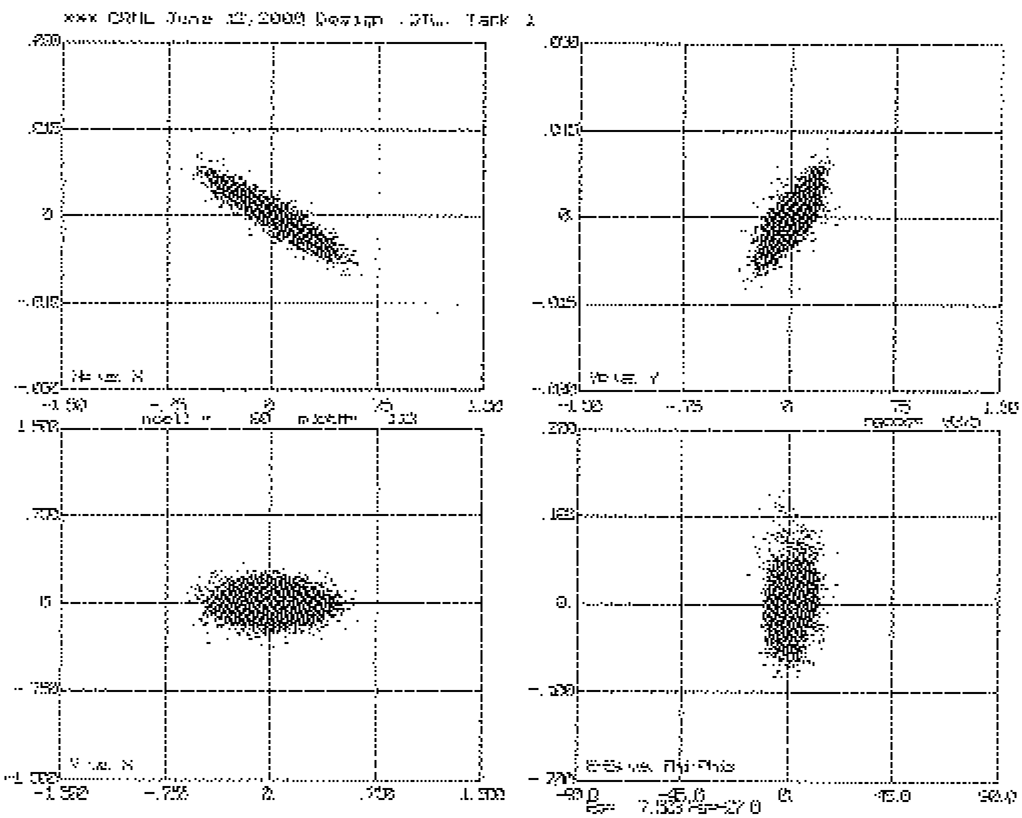

Figure 8 -- Tank 1 output phase-space distributions using the RFQ distribution.